Solid-state NMR as a probe of anion binding: Molecular dynamics and associations in a [5]polynorbornane bisurea host complexed with terephthalate

ARTICLE *in* PHYSICAL CHEMISTRY CHEMICAL PHYSICS · AUGUST 2015

Impact Factor: 4.49 · DOI: 10.1039/c5cp03628c · Source: PubMed

6 AUTHORS, INCLUDING:

Aditya Rawal

University of New South Wales

33 PUBLICATIONS **452** CITATIONS

SEE PROFILE

James M Hook

University of New South Wales

110 PUBLICATIONS **2,049** CITATIONS

SEE PROFILE

Daniel Gunzelmann

Deakin University

23 PUBLICATIONS **521** CITATIONS

SEE PROFILE

Fred Pfeffer

Deakin University

73 PUBLICATIONS **2,812** CITATIONS

SEE PROFILE

PCCP

PAPER

View Article Online
View Journal | View Issue

Cite this: *Phys. Chem. Chem. Phys.*, 2015, **17**, 22195

Solid-state NMR as a probe of anion binding: molecular dynamics and associations in a [5]polynorbornane bisurea host complexed with terephthalate†

Aditya Rawal,*[a] James M. Hook,[a] Ryan N. Robson,[b] Daniel Gunzelmann,[c] Frederick M. Pfeffer[b] and Luke A. O'Dell*[c]

Received 23rd June 2015,
Accepted 28th July 2015

DOI: 10.1039/c5cp03628c

www.rsc.org/pccp

A range of solid-state NMR techniques is used to characterise a molecular host:guest complex consisting of a [5]polynorbornane bisurea host binding a terephthalate dianion guest. Detailed information is obtained on the molecular dynamics and associations from the point of view of both the host and guest molecules. The formation of the complex in the solid state is confirmed using ^{1}H 2D exchange NMR, and the 180° flipping of the ^{2}H-labelled terephthalate guest and its eventual expulsion from the complex at elevated temperatures are quantified using variable-temperature ^{2}H spin-echo experiments. Two-dimensional ^{1}H–^{13}C HETCOR spectra obtained under fast magic angle spinning conditions (60 kHz) show a high resolution despite the poor crystallinity of the solid complex, and clearly reveal changes in the rigidity of the host molecule when complexed. Short-range intra- and intermolecular ^{1}H–^{1}H proximities are also detected using 2D SQ–DQ correlation methods, providing insight into the molecular packing in the solid phase.

1. Introduction

Anion binding plays a critical role in biological systems, catalysis, medicine, environmental science, supramolecular chemistry and crystal engineering,[1–4] and the design, synthesis and characterisation of anion receptors constitutes a rich and rapidly developing field of research.[5,6] For example, molecular receptors based on urea or thiourea moieties can be designed to selectively bind monatomic or molecular anions in solution through non-covalent interactions such as hydrogen bonds.[7–9] Probing anion complexation in the solid state allows these binding interactions to be studied in depth, providing detailed information on the hydrogen bonding arrangement and the conformational geometry of both the anion and the receptor molecule.[10–14] Single-crystal X-ray diffraction is often used to provide crystal structures that complement solution-state binding studies (most often based on ^{1}H NMR titration experiments).[15–21] Unfortunately, high quality crystals suitable for X-ray evaluation or other diffraction techniques are not easily obtained for the vast majority of host:guest combinations. Furthermore, the host and guest molecules can potentially undergo significant dynamic processes in the solid state. Diffraction methods, like solution-state NMR studies, provide only a time-averaged picture of what may be a highly dynamic system, and any motional processes exhibited by the bound anion could affect the binding strength and are therefore of significant interest.

Solid-state NMR has the capability to provide detailed information on not just molecular structures but also intra- and intermolecular interactions and, in particular, molecular dynamics.[22–28] In their detailed NMR studies of a solid-state molecular tweezer complex, Spiess *et al.* demonstrated that the dynamics of a guest molecule can be quantified in terms of rotational rates and geometries, and also used Hartree–Fock calculations to study the effects of intermolecular ring-currents on the ^{1}H chemical shifts.[29–31] These authors had the distinct advantage of a pre-determined crystal structure for their system, which was used to guide the NMR analysis and quantum chemical calculations. In principle, however, solid-state NMR can provide a wealth of information on supramolecular systems for which no crystal structure information is available, particularly when solution-state NMR results are incorporated to aid peak assignment and to identify potential binding arrangements. Indeed, even disordered (non-crystalline) systems can be studied in detail using this versatile technique.

[a] *Mark Wainwright Analytical Centre, University of New South Wales, NSW 2052, Australia. E-mail: a.rawal@unsw.edu.au; Tel: +61-2-9385-4616*
[b] *Centre for Chemistry and Biotechnology, School of Life and Environmental Sciences, Deakin University, Geelong Waurn Ponds Campus, Victoria 3220, Australia*
[c] *Institute for Frontier Materials, Deakin University, Geelong Waurn Ponds Campus, Victoria 3220, Australia. E-mail: luke.odell@deakin.edu.au; Tel: +61-3-5227-3076*

† Electronic supplementary information (ESI) available: Synthesis details for **1**, ^{1}H solution NMR titration data, X-ray powder diffraction data, additional NMR spectra and ^{2}H NMR simulations. See DOI: 10.1039/c5cp03628c

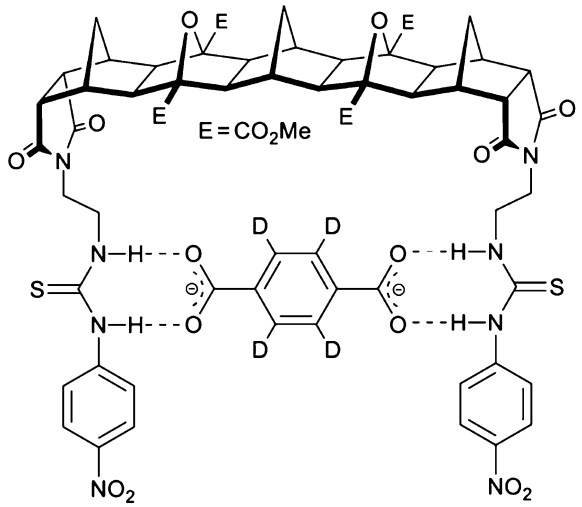

Fig. 1 Structure of the [5]polynorbornane bisurea host (**1**) and d_4-terephthalate guest (the two tetramethylammonium counterions are not shown).

Highly pre-organised, fused [*n*]polynorbornane frameworks have been used in a number of supramolecular settings[32–40] and hosts such as **1** (Fig. 1) are well suited for study by NMR techniques as they are symmetric (C_{2v} and σ), and their binding behaviour with a range of guest anions in solution has been studied in depth.[41–45] Indeed, terephthalate has been found to bind strongly to **1** ($\log K_{1:1} > 5$) in DMSO,[46,47] however, solid-state characterisation of the anion complex has thus far remained elusive, and very little is known about the dynamics of either the host or guest molecules when complexed. In this study, a range of solid-state NMR techniques has been used to characterise this complex in the absence of a crystal structure, from the point of view of both the host and guest species. High resolution, two-dimensional ^{1}H–^{1}H and ^{1}H–^{13}C correlation spectra have been obtained using fast magic angle spinning, providing information on the structure and rigidity of the system, while ^{2}H NMR reveals quantitative information on the dynamics of the bound terephthalate dianion.

2. Experimental

2.1 Sample preparation

The synthetic procedure previously described by Pfeffer and Lowe[46,47] was used in the synthesis of the [5]polynorbornane bisurea host **1** (see ESI† for details, including for the preparation of the bis(tetramethylammonium) (TMA) d_4-terephthalate salt). The **1**:(d_4-)terephthalate complexes, in both unlabelled and ^{2}H labelled form, were prepared by dissolving and stirring equimolar amounts of **1** and bis(TMA) (d_4-)terephthalate in THF for 24 h then removing the solvent under reduced pressure. The resulting solid powder was further dried under high vacuum for 48 h prior to characterisation.

2.2 X-ray powder diffraction

X-ray diffractograms were obtained from powder samples of the solid host **1**, the **1**:terephthalate complex and the bis(TMA) d_4-terephthalate salt using a Panalytical X'Pert Powder diffractometer in Bragg–Brentano geometry (reflection mode). It was set up using a copper anode (CuK_α, λ = 0.1542 nm), a graphite monochromator and a high-speed line PIXcel detector. The diffractograms were collected over an angle range of 7–36° at a scan rate of 60 s per step or over 7–70° at 15 s per step, with a step size of 0.013°.

2.3 Solid-state NMR spectroscopy

^{2}H solid-state NMR spectra were obtained from the **1**:d_4-terephthalate complex at 11.7 T (^{2}H Larmor frequency = 76.8 MHz) using a Bruker Avance III NMR spectrometer and a 5 mm static double-resonance probe. A solid echo (90–τ–90) pulse sequence was used with a ^{2}H 90° pulse width of 7 μs, τ = 20 μs and a ^{1}H decoupling field of approximately 40 kHz. The sample temperature was calibrated using the ^{207}Pb signal from a powder sample of lead nitrate.[48,49] The recycle delays used were 2 s for the complex (1000 scans acquired per spectrum) and 20 s for bis(TMA) d_4-terephthalate (80 scans per spectrum). Due to the dominance of the first-order quadrupolar interaction, the ^{2}H powder patterns are inherently symmetric, allowing the spectra to be added to their own mirror image (*i.e.*, frequency scale reversed) after Fourier transformation and providing an increase in the signal to noise ratio of $\sqrt{2}$.

The ^{2}H spectra were simulated using the NMR WEBLAB v5.0.[50] Due to the symmetry of the d_4-terephthalate dianion, the four ^{2}H electric field gradient (EFG) tensors were assumed to be equivalent, axially symmetric and oriented parallel to the C–^{2}H bond. The simulations therefore only involved a single ^{2}H tensor oriented with the largest principal component at 60° relative to the 180° flip axis, *i.e.*, θ = 60° and ϕ = 180° in the WEBLAB's cone model (see Fig. 3a in Hansen *et al.*[51]). Powder averaging was applied to account for all possible orientations of the flip axis. A broad log-Gaussian distribution in the jump rate (4 decades FWHM) was necessary to include in all ^{2}H simulations to accurately reproduce the experimental line shapes. As discussed by Hansen *et al.*,[51] such a distribution can reflect variations in the activation energy for the jump mechanism, *e.g.*, due to the presence of structural disorder. The slow motion limit ^{2}H quadrupolar coupling constants were measured as C_Q = 177 kHz for the **1**:d_4-terephthalate complex and 181 kHz for the bis(TMA) d_4-terephthalate salt, with the asymmetry parameter η_Q = 0.01 in both cases. It should be noted that the experimental spectra show reduced signal intensities at the outer edges (the "feet" of the powder patterns) due to the limited excitation bandwidth of the pulses used. This problem can potentially be circumvented through the use of frequency-swept pulses or piece-wise acquisition methods, however these methods can lead to line shape distortions[52] or significant increases in acquisition times. When matching the simulations (which assume uniform excitation) to the experimental patterns, emphasis was therefore placed on the shape of the central regions, particularly the relative heights of the inner discontinuities.

^{1}H–^{13}C heteronuclear correlation and ^{1}H–^{1}H homonuclear correlation spectra were obtained from the **1**:terephthalate complex at 16.4 T (^{1}H and ^{13}C Larmor frequency of 700 MHz

and 175 MHz respectively) using a Bruker Avance III NMR spectrometer and a 1.3 mm magic angle spinning (MAS) double resonance probe. Approximately 5 mg of sample was packed in a 1.3 mm MAS rotor for measurement. The spectra were acquired at 60 kHz MAS with temperature regulation to offset the MAS heating effects, which yielded a sample temperature of approximately 55 °C. The ^{1}H 90° pulse width was 1.7 μs and continuous wave ^{1}H decoupling of 6 kHz was used. For the HETCOR experiment, ^{1}H to ^{13}C cross polarization was achieved *via* a 3 ms contact pulse. The contact pulse amplitude on the ^{1}H channel was ramped from 70 to 100% to minimize variation in transfer efficiency due to mismatch of the cross-polarisation condition. The cross-polarization conditions were optimized to a 200 kHz RF field strength on the ^{1}H channel and a 120 kHz field on the ^{13}C channel. This would correspond closely to the zero-quantum cross-polarization (ZQCP) in the high power regime as described by Laage *et al.*[53] The 2D dataset was acquired by collecting 32 transients in the indirect domain with increments of 50 μs in the ^{1}H evolution time. The 2D ^{1}H–^{1}H single quantum–double quantum (SQ–DQ) correlation spectra were acquired using the back to back (BABA) excitation scheme[54] with 4 rotor periods of double quantum excitation and reconversion. The 2D data set was acquired by collecting 256 transients in the indirect domain with increments of one rotor period for the ^{1}H evolution. The 2D ^{1}H–^{1}H SQ–SQ correlation experiments (2D exchange) were acquired with ^{1}H spin diffusion "mixing times" of 100 ms to 1 s. Where needed, a 9 ms ^{1}H-T_2 filter period was inserted to spectrally "edit out" the rigid components prior to the ^{1}H evolution in the indirect domain. The data set was acquired by collecting 256 transients in the indirect domain with increments of 80 μs in the ^{1}H evolution time.

3. Results and discussion

3.1 Long range ordering in the host and complex

The X-ray powder diffraction patterns obtained from the solid host compound **1** and the **1**:terephthalate complex are shown in Fig. 2, expanded around the low angle region (see ESI† for the full 2θ range as well as the pattern obtained from the bis(TMA) d_4-terephthalate salt). No peaks were observed at all for the pure host in the solid state, indicating an absence of long range ordering. For the **1**:terephthalate complex, a number of peaks were visible, indicating that the presence of the terephthalate dianion results in a greater extent of ordering in the solid phase. However, these peaks are rather broad, suggesting either that the crystals are somewhat disordered, or that the dimensions of the crystalline domains are on the order of tens of nm or less. In either case, such a sample is not amenable to study using diffraction techniques. Other methods such as solid-state NMR, which can identify intra- and inter-molecular associations in disordered samples, are exceptionally valuable in such cases.

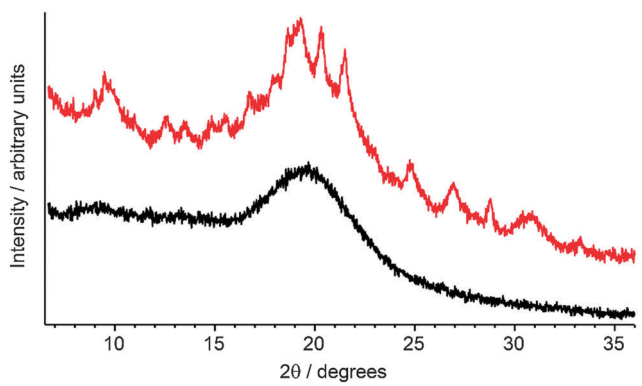

Fig. 2 X-ray powder diffraction patterns obtained from the host compound **1** (black) and the **1**:terephthalate complex (red). See ESI† for the full 2θ range.

3.2 Confirmation of 1:terephthalate complex formation

Evidence for the molecular-level mixing of **1** and the terephthalate dianion in the solid state is provided by the 2D ^{1}H–^{1}H spin diffusion NMR spectra shown in Fig. 3. In these spectra, off-diagonal peaks arise for two distinct ^{1}H environments if magnetisation is exchanged between them during a variable spin diffusion time. Increasing the spin diffusion time allows the exchange to occur between more distant sites. The 2D spectrum without any spin diffusion time yields a diagonal ridge (*i.e.*, only auto-correlation peaks) as shown in the ESI† (Fig. S14).

For the case of the solid bisurea host **1**, at 60 kHz MAS a 100 ms spin diffusion time is sufficient for complete exchange of magnetization among the different ^{1}H sites with the cross-peaks observed between all the sites (Fig. 3a). In order to observe ^{1}H spin diffusion between the host and the guest molecule in the complex, it is necessary to spectrally edit the overlapping ^{1}H signals arising due to host–host and guest–guest correlations. This is made possible by differences in the dynamics of the various species, as will be discussed in detail in the following sections. As the terephthalate and TMA ions are more mobile than **1**, the signals from those species can be selected using a ^{1}H-T_2 filter (see ESI,† Fig. S14). With a 1 s spin diffusion time, cross-peaks appear between the TMA and **1** as seen in Fig. 3b(iii), indicating their close proximity. Interestingly, even at this long spin diffusion time a complete exchange of signals between the TMA and **1** is not observed, and no cross-peaks are observed between the terephthalate and the host molecule. This can be explained on the basis of the difference in the mobility and size of the TMA and terephthalate ions. As demonstrated in the following section, the terephthalate ion undergoes relatively fast rotational jumps in the binding cleft of host **1**, suppressing the spin diffusion contact between itself and the host. The bulkier TMA cations will exhibit slower dynamics while remaining in close proximity to the host to counter the charge on the terephthalate.

3.3 Dynamics of the terephthalate dianion

Detailed and quantitative information on the molecular dynamics occurring in macromolecular supramolecular systems have been obtained by means of ^{2}H solid-state NMR studies, primarily from the point of view of aromatic linker groups in

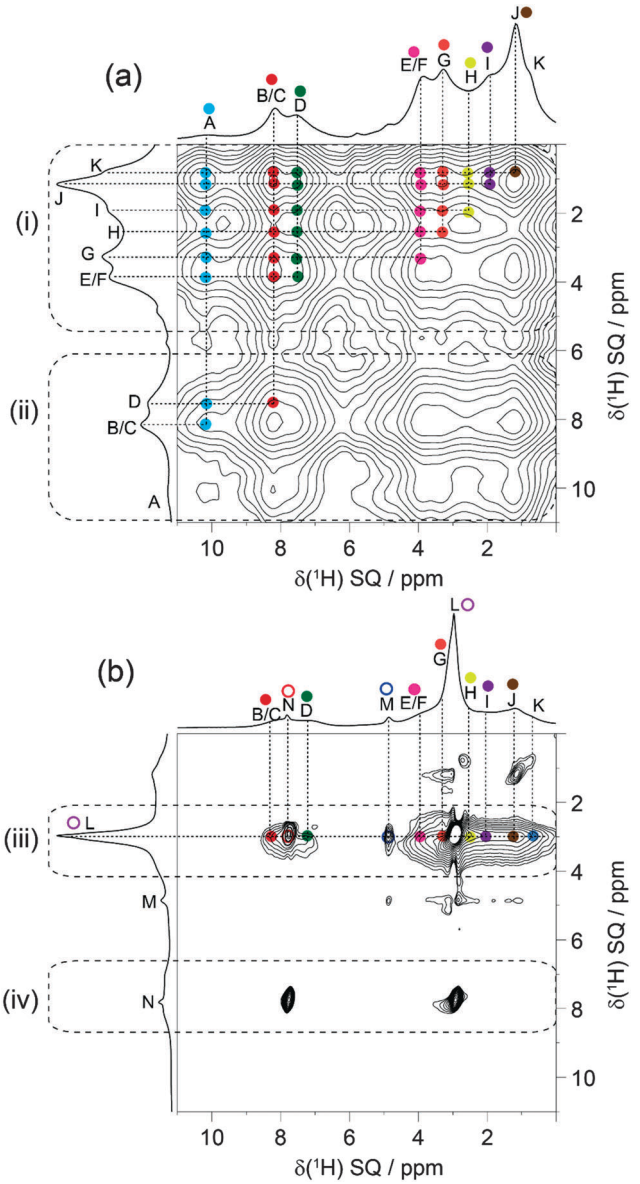

Fig. 3 2D ^{1}H spin diffusion spectra of (a) the host compound **1** and (b) the **1**:terephthalate complex. The dotted boxes identify the spectral region for (i) the backbone of **1**, (ii) the arms of **1**, (iii) the TMA counter ions and (iv) the terephthalate guest. The spectrum in (a) was acquired with a 34 μs ^{1}H-T_2 filter and 100 ms spin diffusion time, while (b) was acquired with a 9 ms ^{1}H-T_2 filter and 1 s spin diffusion time. The TMA counter ion peak is labelled L, the water peak is labelled M and the terephthalate peak is labelled N. The remaining peak assignments are as described in Fig. 6. The coloured circles indicate the cross peaks among the different sites. For spectrum (a), which is symmetric about the slope 1 diagonal, the correlation peaks below the diagonal are not marked. Spectrum (b) is asymmetric due to the 9 ms ^{1}H T_2 filter, and only shows the cross-peaks from TMA (site L) to the host.

porous host materials. For example, Kolokolov *et al.* have used ^{2}H NMR to observe correlations between linker group dynamics and the rigidity of the framework,[55] as well as the pore opening size,[56] and Loeb and co-workers studied the dynamics of interlocked components in metal organic frameworks.[24–26] Similarly, ^{2}H NMR can be used to monitor the incorporation of guest molecules into a host structure, which can have a significant influence on the motional rates and their activation energies.[57–59] It is therefore surprising that apart from the previously mentioned work of Spiess and co-workers,[29–31] ^{2}H solid-state NMR studies of molecular host:guest complexes and anion binding systems are scarce.

The use of a deuterium-labelled terephthalate guest molecule as shown in Fig. 1 enables a direct probe of the temperature-dependent guest dynamics (with motional rates $>10^{4}$ s^{-1}) by ^{2}H solid-state NMR. Solution-state NMR titrations showed no apparent difference in the binding of deuterated and undeuterated terephthalate by **1** (see ESI†). Selected ^{2}H solid-state NMR spectra obtained from the **1**:d_4-terephthalate complex at various temperatures are shown in Fig. 4a (see ESI† for all ^{2}H NMR spectra and simulations). As the sample temperature increases, the shape of the broad ^{2}H NMR powder pattern changes due to the presence of anisotropic ^{2}H transverse relaxation induced by the reorientation of the C–^{2}H bonds.[60] The presence of a non-axially symmetric ^{2}H powder pattern in the fast motion limit implies that the molecule is not freely rotating but rather is undergoing flips between two or more fixed orientations. The hydrogen bonding arrangement of the complex, combined with the planar nature of the terephthalate dianion, would suggest a 180° flip of the molecule about its long axis as the most likely mechanism. The effect of this motion on the ^{2}H NMR spectrum was simulated with a log-Gaussian distribution in jump rates required in order to accurately reproduce the experimental line shapes over the full range of temperatures studied (−40 to 100 °C). This log-Gaussian distribution is a key indicator of the presence of structural disorder within the complex,[51] consistent with the X-ray powder diffraction data discussed above.

The ^{2}H simulations also allow the extraction of an activation energy of 61 ± 2 kJ mol^{-1} for the terephthalate flipping mechanism within the complex *via* an Arrhenius plot (Fig. 4b). The pure, solid bis(TMA) d_4-terephthalate salt was also studied with no host present, and was found to exhibit the same 180° flipping process but with a significantly higher activation energy (87 ± 6 kJ mol^{-1}). This difference can be attributed to a greater steric hindrance in the latter system. While the crystal structure of the **1**:terephthalate complex is unknown (and may be relatively disordered), it can be inferred that the terephthalate dianion positions within the relatively large cleft of the host molecule, and its rotation is therefore less sterically hindered than in the TMA salt form, in which the molecules are likely to be more closely packed. Indeed, Spiess has described this experimental approach as a "probe of free volume",[60] and activation energies reported for terephthalate ring flips in polymers can vary between 24 and 77 kJ mol^{-1} depending on the local structural environment.[61,62] However, a more recent ^{2}H NMR study of the metal organic framework MOF-5 containing d_4-terephthalate groups as the organic linkers, reported a flip activation energy of 47 kJ mol^{-1}, much higher than expected given the almost complete absence of steric hindrance in this structure.[63] The authors discussed this observation in terms of ordering. The inherent disorder in a polymer can provide a distribution of high-energy conformations for the terephthalate groups (as well as other dynamic modes such as small angle flips), which can lower

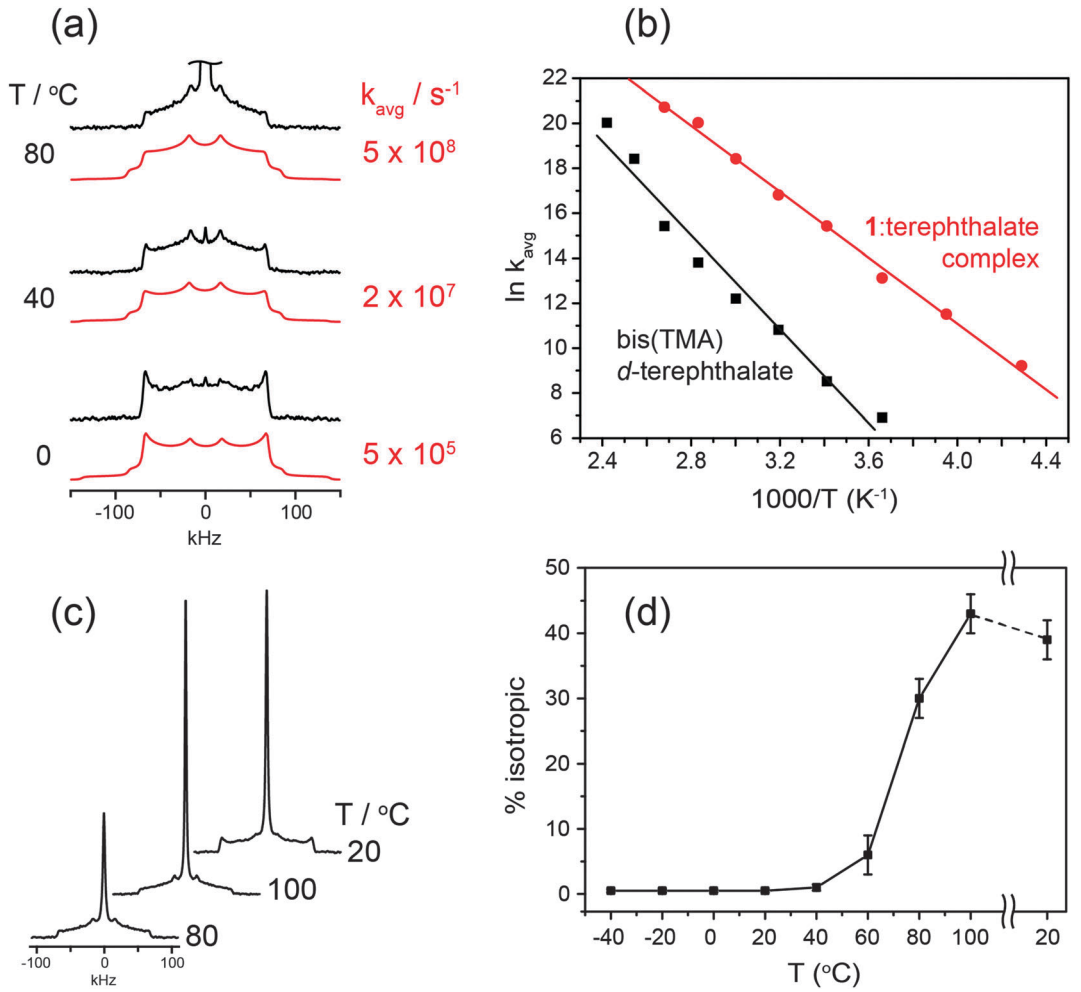

Fig. 4 (a) ^{2}H NMR spectra obtained from the **1**:terephthalate complex at select temperatures shown (black) and line shapes simulated by modelling a 180° flip of the guest molecule about its long axis at the average jump rates k_{avg} indicated (red). (b) Arrhenius plots of k_{avg} for the complex (red) and bis (tetramethylammonium) d_4-terephthalate (black) with linear fits. (c) ^{2}H NMR spectra from the complex obtained at the temperatures indicated, with the isotropic peak visible. (d) Percentage of isotropically rotating terephthalate component in the complex as a function of temperature (right-most 20 °C data point obtained after cooling from 100 °C).

the energy required for a flip to occur. In contrast, the flipping in MOF-5 occurs between two very well-defined, low-energy conformations representing deep valleys in the energy landscape. For the **1**:terephthalate complex, the observation of a distribution in flip rates suggests that some variation in terephthalate conformations is present (again, consistent with the disordered nature of the sample), but the higher activation energy than for MOF-5 suggests that local steric hindrance dominates the energetics, presumably due to the packing of the complex units and TMA counterions.

The ^{2}H NMR spectra obtained at higher temperatures also show a narrow peak (width $\approx$ 1.3 kHz) in the centre of the spectra (Fig. 4c). This component arises from terephthalate molecules undergoing isotropic rotation.[60] The percentage of this component, measured by deconvolution of the NMR spectral intensities, is plotted against temperature in Fig. 4d. While a very small isotropic component (<1%) exists even at the lowest temperatures studied, a significant increase occurs at approximately 60 °C and by 100 °C this constitutes around 40% of the signal. Crucially, upon cooling back to 20 °C this isotropic peak remains unchanged while the shape of the broad powder pattern returns to its original state. Exchange of the deuterons with the protons of the TMA cation (itself likely to be undergoing isotropic rotation) can be ruled out as this was not observed in the bis(TMA) d_4-terephthalate salt even at 140 °C (see ESI†). This isotropically rotating fraction likely corresponds to terephthalate molecules that are no longer bound within the host molecule, and that presumably exist within a separate phase that also contains the TMA co-cations to charge balance. However, its ^{2}H NMR signature does not match that of the pure bis(TMA) d_4-terephthalate sample (see ESI†). As the dianion is undergoing isotropic rotational dynamics, this phase could be plastic crystalline in nature.[64] Nevertheless, these results clearly indicate that elevated temperatures cause a significant percentage of the guest population to become displaced from the host.

3.4 Dynamics of the [5]polynorbornane host

Due to its much larger size, the solid-state dynamics of the [5]polynorbornane host molecule are expected to be significantly slower than those of the terephthalate ion and as a consequence are not as conveniently probed by ^{2}H NMR. However, motional dynamics occurring on the order of kHz can have a significant impact on ^{1}H–^{13}C dipolar coupling interactions, which are readily probed by 2D ^{1}H–^{13}C heteronuclear correlation spectroscopy (HETCOR). Under ultrafast (60 kHz) magic angle spinning (MAS) conditions, weaker (long range) dipolar couplings are averaged out, effectively amplifying the differences in ^{1}H–^{13}C dipolar couplings for proximate sites in the structure. As a result, the efficiency of the dipolar-mediated (through space) polarization transfer from ^{1}H to ^{13}C can be strongly influenced by subtle changes in molecular motion.

The ^{1}H–^{13}C HETCOR solid-state spectra of the [5]polynorbornane host compound **1** alone and the **1**:terephthalate complex are shown in Fig. 5a and b respectively. It is worth noting that these spectra were acquired without isotropic enrichment and using only 5 mg of sample. In the case of the [5]polynorbornane host without the terephthalate guest present, correlation peaks from the norbornane backbone are well resolved, indicating relatively strong ^{1}H–^{13}C dipolar couplings as would be expected in this rigid section of the molecule. However, the signals from the thiourea and nitrobenzene groups (the arms of the molecular cleft) are much weaker, reflecting weak ^{1}H–^{13}C dipolar couplings indicative of greater mobility of these groups, likely a combination of aryl ring librations and bending of the molecular arms. For the **1**:terephthalate complex, strong signals from the nitrobenzene groups are visible in addition to the signals from the norbornane framework. This clearly shows that the binding of the terephthalate suppresses the motion of the nitrobenzene groups, making the arms more rigid.

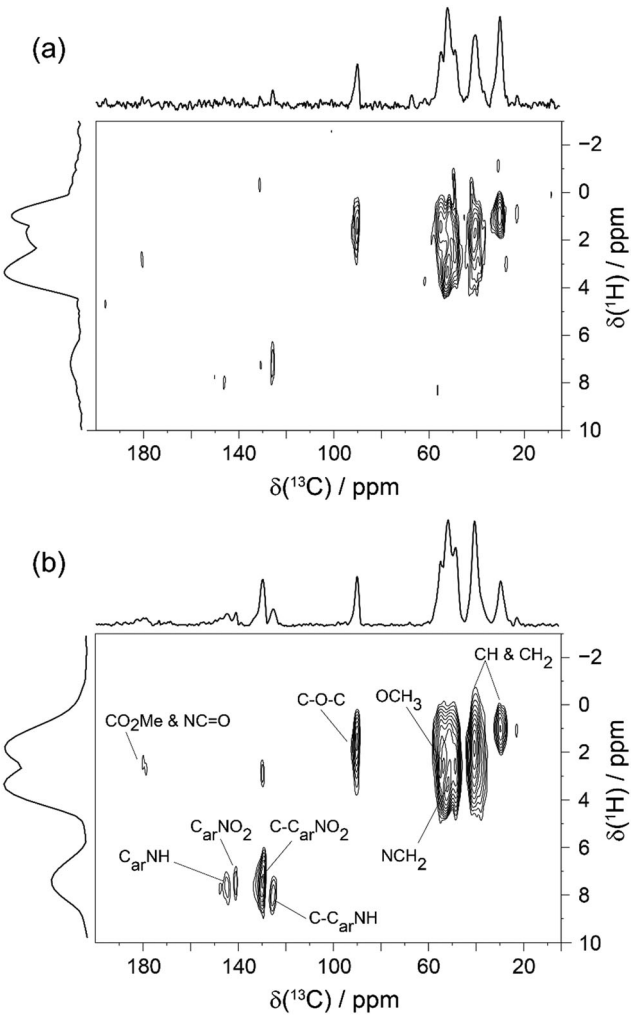

Fig. 5 ^{1}H–^{13}C HETCOR solid-state NMR spectra of (a) the host compound **1** and (b) its complex with terephthalate, obtained at 16.4 T and 60 kHz MAS. Peak assignments are shown in (b). The ^{1}H and ^{13}C projections are plotted at the left and top of each spectrum. C_{ar} = aromatic carbon sites.

It should also be noted that the HETCOR experiments were performed at a sample temperature of 55 ± 5 °C due to the frictional heating caused by the fast sample rotation. At this temperature, the guest molecules that are still bound within the complex (>90% according to Fig. 4d) are undergoing ring flips at the rate of $k_{avg} \approx 10^{8}$ s^{-1} and would have negligible ^{1}H–^{13}C dipolar couplings under the ultrafast MAS conditions. This explains the absence of signals from the guest molecule in these spectra. The combination of a highly dynamic guest ion inside a rigid host molecule can be understood by considering the structure of the complex in Fig. 1. The terephthalate dianion forms hydrogen bonds with the thiourea groups on either side, which lock the thiourea arms in place. Due to the symmetry of the guest molecule, rapid 180° flips about the long axis of the terephthalate as indicated by the ^{2}H NMR will result in no net change to these hydrogen bonds. However, as the ^{2}H NMR clearly shows, higher temperatures can disrupt these interactions and cause the guest to be expelled from the complex.

3.5 Local ordering within the complex

While information regarding the long range ordering of **1** and its complex in the solid state is challenging to obtain due to the lack of sharp diffraction peaks observed in Fig. 2, it is possible to gain insight into the local ordering using high resolution ^{1}H MAS NMR. Fig. 6a and b show 2D ^{1}H single quantum double quantum (SQ–DQ) correlation spectra for **1** and the **1**:terephthalate complex respectively, with the 1D ^{1}H NMR spectra shown at the top. Peak assignments are shown in Fig. 6c. Differences in the 1D ^{1}H NMR spectra confirm the variation in the dynamics of the host molecules observed in the HETCOR experiment. For example, the motionally narrowed ^{1}H signals of the aromatic protons (B and D) and the CH_2 protons on the host arms (E) in **1** are broadened due to reduced mobility (and therefore increased dipolar couplings) in the **1**:terephthalate complex. Additionally, an intense peak (L) arising from the TMA cations in the complex is visible in Fig. 6b. This peak is relatively sharp, suggesting that these ions are dynamic.

The presence of SQ–DQ cross peaks in these 2D spectra (highlighted using red or blue dashed lines) reveal ^{1}H–^{1}H proximities in these systems by means of through-space dipolar

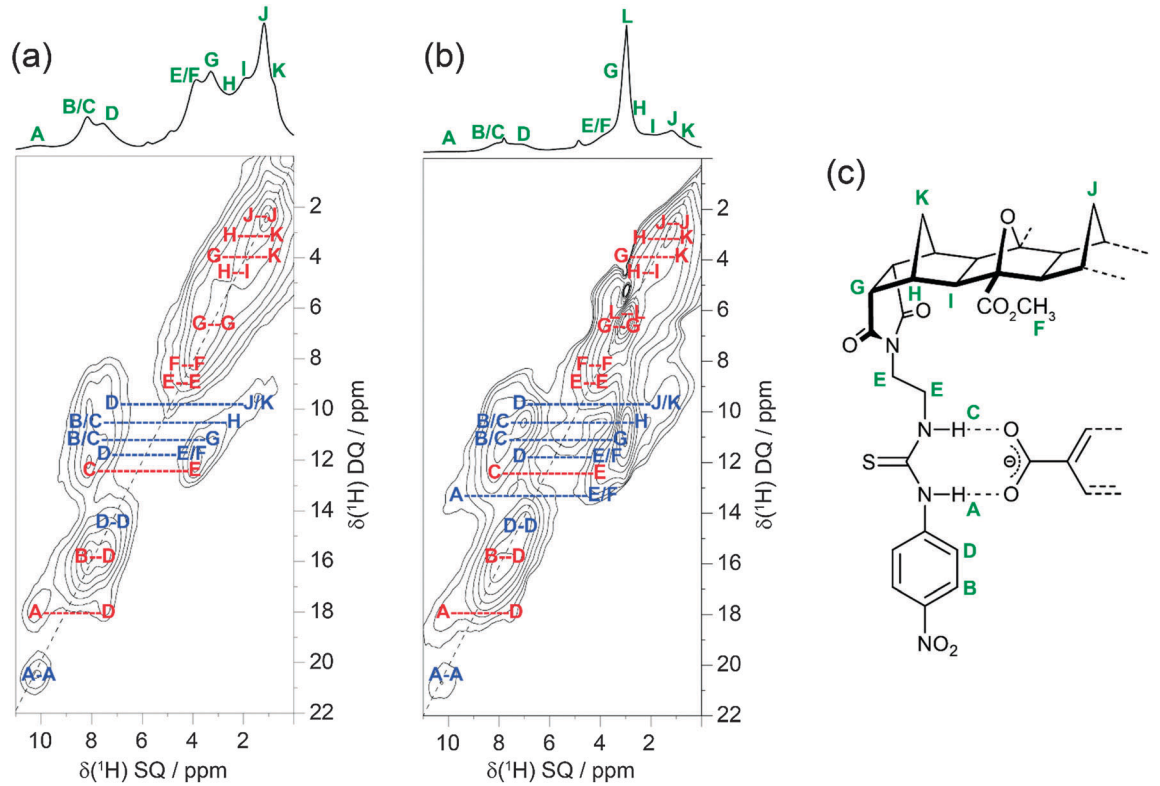

Fig. 6 2D ^{1}H single-quantum double-quantum (SQ–DQ) correlation spectra of (a) the host compound **1** and (b) the **1**:terephthalate complex. Pairs of cross peaks are highlighted in red (intramolecular proximities) and blue (intermolecular proximities). The ^{1}H peaks shown at the top of each spectrum are assigned to the molecular sites as indicated in (c). Peak L arises from the protons on the tetramethylammonium cation.

couplings. As this interaction only occurs for sites in close proximity, correlations observed for nuclei that are distant in the molecular structure must correspond to intermolecular associations. The correlation peaks between 1 and 9 ppm along the DQ dimension represent the intramolecular ^{1}H–^{1}H proximities within the [5]polynorbornane backbone of **1**. Additional intramolecular proximities between A–D, B–D, C–E and E–E are also observed arising from the arms of the host molecule. These correlations are illustrated with red dashed lines. Intermolecular proximities between neighbouring molecules are also evident and are highlighted by blue dashed lines. These provide insight into the local ordering in the system, *i.e.*, the packing of the **1** or **1**:terephthalate units. In both systems, strong correlations are observed between B–G, B–H, D–J and D–K, indicating intermolecular proximities between the aromatic groups of the host arms and the [5]polynorbornane backbone.

There are also observable differences between the ^{1}H–^{1}H correlations in the two systems. For example, a strong A–A autocorrelation peak for the host compound **1** (Fig. 6a) indicates inter-molecular hydrogen bond interactions for the thiourea NH species proximal to the aromatic ring. This A–A autocorrelation peak is significantly weaker for the **1**:terephthalate complex, while the peaks for the A–E/F, B–G, B–H and D–J proximities are observed to be stronger in intensity than in the host system (Fig. 6b). The weakening of the A–A peak indicates disruption of the intermolecular N–H interactions due to the presence of the terephthalate guest, as one would expect, while the increased rigidity of **1** in the complex would be expected to enhance the intensity of the intermolecular correlation peaks. No clear correlation peak was observed between **1** and the TMA or terephthalate species, which is likely due to the dynamics of these molecules under the experimental conditions used (55 °C).

4. Conclusions

The solid but poorly crystalline [5]polynorbornane:terephthalate host:guest complex was not amenable to diffraction studies but has been successfully characterised using a judicious choice of solid-state NMR techniques. ^{1}H spin exchange experiments showed a transfer of magnetisation between the host molecule and the TMA counterions, providing direct evidence for the molecular-level mixing of the host and the ionic species. ^{2}H NMR was used to probe the dynamics of the labelled guest molecule, allowing the measurement of the activation energy for the terephthalate's 180° flipping mechanism (61 ± 2 kJ mol^{-1}). This value is higher than that measured for the same mechanism in a metal organic framework but lower than that in a solid terephthalate salt, indicating an intermediate level of steric hindrance. The ^{2}H NMR also showed the irreversible expulsion of the guest molecule at higher temperatures. Two-dimensional, high-speed MAS ^{1}H–^{13}C HETCOR spectra of the solid host with and without the guest molecule present were sufficiently sensitive to show that the binding of the guest

molecule *via* hydrogen bonding with the thiourea groups results in the molecular arms of the host becoming more rigid. Finally, insights into the packing of the host and complex units in the solid state was provided by 2D ^{1}H–^{1}H NMR spectra, which show intermolecular proximities between the molecular arms and polynorbornane backbone.

This work has clearly demonstrated the utility of solid-state NMR spectroscopy as a means to characterise anion hosts interacting with their target guests, and as a means to probe the structure and dynamics of poorly crystalline supramolecular host:guest systems in general. It is hoped that this will encourage more widespread use of solid-state NMR to probe intermolecular binding, motion and rigidity in solid supramolecular assemblies, particularly in systems that are not highly crystalline and are therefore unsuitable for diffraction methods.

Acknowledgements

The Australian Research Council is also acknowledged for funding Deakin University's Magnetic Resonance Facility through LIEF grant LE110100141. FP thanks the ARC (DP140100227) and the Centre for Chemistry and Biotechnology for funding aspects of this work. The Mark Wainwright Analytical Centre at UNSW is acknowledged for access to the solid state NMR spectrometers funded through ARC LIEF LE0989541.

References

1 P. D. Beer and P. A. Gale, *Angew. Chem., Int. Ed.*, 2001, **40**, 486.
2 D. B. Varshey, J. R. G. Sander, T. Friščič and L. R. MacGillivray, in *Supramolecular Chemistry: From Molecules to Nanomaterials*, ed. J. W. Steed and P. A. Gale, John Wiley & Sons, Ltd, 2012, pp. 9–25.
3 G. R. Desiraju, *Angew. Chem., Int. Ed. Engl.*, 1995, **34**, 2311.
4 T. D. Ashton, K. A. Jolliffe and F. M. Pfeffer, *Chem. Soc. Rev.*, 2015, **44**, 4547.
5 P. A. Gale, N. Busschaert, C. J. E. Haynes, L. E. Karagiannidis and I. L. Kirby, *Chem. Soc. Rev.*, 2014, **43**, 205.
6 N. Busschaert, C. Caltagirone, W. V. Rossom and P. A. Gale, *Chem. Rev.*, DOI: 10.1021/acs.chemrev.5b00099.
7 V. Amendola, L. Fabbrizzi and L. Mosca, *Chem. Soc. Rev.*, 2010, **39**, 3889.
8 A.-F. Li, J.-H. Wang, F. Wang and Y.-B. Jiang, *Chem. Soc. Rev.*, 2010, **39**, 3729.
9 V. B. Bregović, N. Basarić and K. Mlinarić-Majerski, *Coord. Chem. Rev.*, 2015, **295**, 80.
10 Y. Inokuma, M. Kawano and M. Fujita, *Nat. Chem.*, 2011, **3**, 349.
11 J. K. Klosterman, Y. Yamauchi and M. Fujita, *Chem. Soc. Rev.*, 2009, **38**, 1714.
12 K. Harris, D. Fujita and M. Fujita, *Chem. Commun.*, 2013, **49**, 6703.
13 J. F. Ayme, J. E. Beves, D. A. Leigh, R. T. McBurney, K. Rissanen and D. Schultz, *Nat. Chem.*, 2012, **4**, 15.
14 M. R. Chierotti and R. Gobetto, *Chem. Commun.*, 2008, 1621.
15 P. Byrne, D. R. Turner, G. O. Lloyd, N. Clarke and J. W. Steed, *Cryst. Growth Des.*, 2008, **8**, 3335.
16 C. A. Johnson, O. B. Berryman, A. C. Sather, L. N. Zakharov, M. M. Haley and D. W. Johnson, *Cryst. Growth Des.*, 2009, **9**, 4247.
17 I. Ravikumar, P. S. Lakshminarayanan, M. Arunachalam, E. Suresh and P. Ghosh, *Dalton Trans.*, 2009, 4160.
18 N. K. Beyeh, M. Cetina and K. Rissanen, *Cryst. Growth Des.*, 2012, **12**, 4919.
19 R. Chutia, S. K. Dey and G. Das, *Cryst. Growth Des.*, 2013, **13**, 883.
20 R. Chutia, S. K. Dey and G. Das, *CrystEngComm*, 2013, **15**, 9641.
21 L. Copey, L. Jean-Gérard, E. Framery, G. Pilet and B. Andrioletti, *Eur. J. Org. Chem.*, 2014, 4759.
22 S. P. Brown and H. W. Spiess, *Chem. Rev.*, 2001, **101**, 4125.
23 L. A. O'Dell and C. I. Ratcliffe, *Quadrupolar NMR to Investigate Dynamics in Solid Materials.*, eMagRes., 2011, pp. 1–16.
24 V. N. Vukotic, K. J. Harris, K. Zhu, R. W. Schurko and S. J. Loeb, *Nat. Chem.*, 2012, **4**, 456.
25 K. Zhu, V. N. Vukotic, C. A. O'Keefe, R. W. Schurko and S. J. Loeb, *J. Am. Chem. Soc.*, 2014, **136**, 7403.
26 K. Zhu, C. A. O'Keefe, V. N. Vukotic, R. W. Schurko and S. J. Loeb, *Nat. Chem.*, 2015, **7**, 514.
27 L. A. O'Dell and C. I. Ratcliffe, *Chem. Commun.*, 2010, **46**, 6774.
28 X. Kong, L. A. O'Dell, V. Terskikh, E. Ye, R. Wang and G. Wu, *J. Am. Chem. Soc.*, 2012, **134**, 14609.
29 S. P. Brown, T. Schaller, U. P. Seelbach, F. Koziol, C. Oschenfeld, F.-G. Klärner and H. W. Spiess, *Angew. Chem., Int. Ed.*, 2001, **40**, 717.
30 C. Oschenfeld, F. Koziol, S. P. Brown, T. Schaller, U. P. Seelbach and F.-G. Klärner, *Solid State Nucl. Magn. Reson.*, 2002, **22**, 128.
31 F.-G. Klärner and B. Kahlert, *Acc. Chem. Res.*, 2003, **36**, 919.
32 M. D. Johnstone, E. K. Schwarze, G. H. Clever and F. M. Pfeffer, *Chem. – Eur. J.*, 2015, **21**, 3948.
33 G. H. Clever, S. Tashiro and M. Shionoya, *Angew. Chem., Int. Ed.*, 2009, **48**, 7010.
34 R. B. Murphy, D. T. Pham, S. F. Lincoln and M. R. Johnston, *Eur. J. Org. Chem.*, 2013, 2985.
35 S. P. Gaynor, M. J. Gunter, M. R. Johnston and R. N. Warrener, *Org. Biomol. Chem.*, 2006, **4**, 2253.
36 P. S. Kearns, B. K. Wells, R. N. Warrener and D. Margetić, *Synlett*, 2014, 1601.
37 F. G. Klärner and T. Schrader, *Acc. Chem. Res.*, 2013, **46**, 967.
38 D. Bier, R. Rose, K. Bravo-Rodriguez, M. Bartel, J. M. Ramirez-Anguita, S. Dutt, C. Wilch, F. G. Klärner, E. Sanchez-Garcia, T. Schrader and C. Ottmann, *Nat. Chem.*, 2013, **5**, 234.
39 T. D. M. Bell, K. A. Jolliffe, K. P. Ghiggino, A. M. Oliver, M. J. Shephard, S. J. Langford and M. N. Paddon-Row, *J. Am. Chem. Soc.*, 2000, **122**, 10661.
40 N. Darwish, I. Díez-Pérez, P. Da Silva, N. Tao, J. J. Gooding and M. N. Paddon-Row, *Angew. Chem., Int. Ed.*, 2012, **51**, 3203.

41 A. J. Lowe, B. M. Long and F. M. Pfeffer, *Chem. Commun.*, 2013, **49**, 3376.
42 A. J. Lowe, B. M. Long and F. M. Pfeffer, *J. Org. Chem.*, 2012, **77**, 8507.
43 B. M. Long and F. M. Pfeffer, *Chem. – Asian J.*, 2014, **9**, 1091.
44 M. D. Johnstone and F. M. Pfeffer, *Supramol. Chem.*, 2014, **26**, 202.
45 F. M. Pfeffer, P. E. Kruger and T. Gunnlaugsson, *Org. Biomol. Chem.*, 2007, **5**, 1894.
46 A. J. Lowe and F. M. Pfeffer, *Chem. Commun.*, 2008, 1871.
47 A. J. Lowe and F. M. Pfeffer, *Org. Biomol. Chem.*, 2009, **7**, 4233.
48 A. Bielecki and D. P. Burum, *J. Magn. Reson.*, 1995, **116**, 215.
49 L. C. M. van Gorkom, J. M. Hook, M. B. Logan, J. V. Hanna and R. E. Wasylishen, *Magn. Reson. Chem.*, 1995, **33**, 791.
50 V. Macho, L. Brombacher and H. W. Spiess, *Appl. Magn. Reson.*, 2001, **20**, 405.
51 M. R. Hansen, R. Graf and H. W. Spiess, *Acc. Chem. Res.*, 2013, **46**, 1996.
52 L. A. O'Dell and R. W. Schurko, *J. Am. Chem. Soc.*, 2009, **131**, 6658.
53 S. Laage, J. R. Sachleben, S. Steuernagel, R. Pierattelli, G. Pintacuda and L. Emsley, *J. Magn. Reson.*, 2009, **196**, 133.
54 M. Feike, D. E. Demco, R. Graf, J. Gottwald, S. Hafner and H. W. Spiess, *J. Magn. Reson.*, 1996, **122**, 214.
55 D. I. Kolokolov, H. Jobic, A. G. Stepanov, V. Guillerm, T. Devic, C. Serre and G. Férey, *Angew. Chem., Int. Ed.*, 2010, **49**, 4791.
56 D. I. Kolokolov, A. G. Stepanov, V. Guillerm, C. Serre, B. Frick and H. Jobic, *J. Phys. Chem. C*, 2012, **116**, 12131.
57 A. Comotti, S. Bracco, T. Ben, S. Qiu and P. Sozzani, *Angew. Chem., Int. Ed.*, 2014, **53**, 1043.
58 A. Comotti, S. Bracco, P. Valsesia, M. Beretta and P. Sozzani, *Angew. Chem., Int. Ed.*, 2010, **49**, 1760.
59 D. I. Kolokolov, A. G. Stepanov and H. Jobic, *J. Phys. Chem. C*, 2014, **118**, 15978.
60 H. W. Spiess, *Colloid Polym. Sci.*, 1983, **261**, 193.
61 A. L. Cholli, J. J. Dumais, A. K. Engel and L. W. Jelinski, *Macromol.*, 1984, **17**, 2399.
62 T. Kawaguchi, A. Mamada, Y. Hosokawa and F. Horii, *Polymer*, 1998, **39**, 2725.
63 S. L. Gould, D. Tranchemontagne, O. M. Yaghi and M. A. Garcia-Garibay, *J. Am. Chem. Soc.*, 2008, **130**, 3246.
64 J. M. Pringle, P. C. Howlett, D. R. MacFarlane and M. Forsyth, *J. Mater. Chem.*, 2010, **20**, 2056.